Disorder effects on the band structure of ZnGeN_{2}: Role of exchange defects

Dmitry Skachkov, Paul C. Quayle, Kathleen Kash, and Walter R. L. Lambrecht

Disorder effects on the band structure of ZnGeN$_2$: the role of exchange defects

Dmitry Skachkov, Paul C. Quayle, Kathleen Kash, and Walter R. L. Lambrecht

Department of Physics, Case Western Reserve University,
10900 Euclid Avenue, Cleveland, OH-44106-7079

The role of exchange defects on the band structure of ZnGeN$_2$ is investigated. Exchange defects are defined through the exchange of cations Zn and Ge starting from the ideal $Pna2_1$ crystal structure, which obeys the local octet rule. Each such exchange creates several nitrogen-centered tetrahedra which violate the local octet rule although overall charge neutrality is preserved. We study several distributions of exchange defects, some with all antisites making up the exchange defect close to each other and with increasing numbers of exchange defects, and others where the two types of antisites Zn$_{Ge}$ and Ge$_{Zn}$ are kept separated from each other. We also compare the results for these models with a fully random distribution of Zn and Ge on the cation sites. We show that for a single-nearest-neighbor exchange defect, the band gap is narrowed by about 0.5 eV due to two effects: (1) the Zn$_{Ge}$ antisites form filled acceptor states just above and merging with the valence band maximum (VBM) of perfect crystal ZnGeN$_2$ and (2) the Ge$_{Zn}$ antisites form a resonance in the conduction band which lowers the conduction band minimum (CBM). When more exchange defects are created, these acceptor states broaden into bands which can lower the gap further. When tetrahedra occur surrounded completely by four Zn atoms, states even deeper in the gap are found localized all near these tetrahedra, forming a separate intermediate band. Finally, for phase segregated Zn$_{Ge}$ and Ge$_{Zn}$ the gap is significantly more reduced, but no separate band is found to occur. The Zn$_{Ge}$ acceptor-like states now form a percolating defect band which is significantly wider and hence reaches deeper into the gap. In all cases, the wave functions near the top of the new VBM remain to some extent localized near the Zn$_{Ge}$ sites. For a fully random case, the gap is even more severely reduced by almost 3 eV. The total energy of the system increases with the number of octet-rule-violating tetrahedra and the energy cost per exchange defect of order 2 eV is quite high.

I. INTRODUCTION

Recently there has been significant new interest in heterovalent ternary nitrides, such as ZnGeN$_2$ and ZnSnN$_2$.[1–8] These materials can formally be thought of as derived from the binary III-N nitrides by replacing the group III by alternatingly a group II element, such as Zn, and a group IV element, such as Ge or Sn. These heterovalent ternaries have properties both similar to and complementary to the well studied III-N semiconductors. However, the additional degree of freedom of having two different valence cations leads to new questions and additional complexity. Most notable is the question of the ordering of the cations.

While the most stable crystal structure found so far for most of these materials has the β-NaFeO$_2$ structure with space group Pna2$_1$, disordered wurtzite-like phases, sometimes identified as having monoclinic structure, have also been reported.[2,3,9,10] Besides the 16-atom unit cell $Pna2_1$ structure, another 8-atom cell with space group $Pmc2_1$ was proposed by Lahourcade *et al.*[4] Both of these structures are unique in that within the overall wurtzite lattice they preserve the octet rule locally in each tetrahedron. That is: each tetrahedron surrounding a N has exactly two group II and two group IV elements such that the charge neutrality is conserved locally. In a recent paper, Quayle *et al.*[8] showed that these are the only two small unit cells that satisfy this rule. Moreover these authors showed that these two structures can be viewed as simply a different stacking of rows of alternating group

II and group IV atoms in the basal plane. This result then suggested that random stackings could also occur and led to a new model for disordered structures which are constrained to preserve the charge neutrality, as opposed to completely random placement of the II and IV atoms on the wurtzite lattice, which would only preserve neutrality globally but not locally. This means, for instance, that some tetrahedra would have one group II and three group IV atoms, which we will call a (1,3) tetrahedron, and be compensated by the opposite (3,1) tetrahedra elsewhere in the structure. In principle, in a fully disordered structure, even (0,4) and (4,0) tetrahedra would occur. In Quayle *et al.*[8] it was shown that a structure with only (1,3) and (3,1) tetrahedra had a significantly higher total energy and lower band gap, and that both structures $Pna2_1$ and $Pmc2_1$, with only (2,2) tetrahedra, had almost the same energy and band gap. On the other hand, it was recently proposed by Feldberg *et al.*[6] that for ZnSnN$_2$ a significantly lower band gap was obtained for "fully" disordered material as compared to the ideal $Pna2_1$ structure. It was however not identified what constitutes "fully disordered", and statistics on the number of each type of tetrahedron in the structure was not provided.

In previous work,[8] we hypothesized that the origin of the decrease of the band gap in disordered structures is related to "wrong" tetrahedra, *i.e.* tetrahedra other than (2,2) that violate the local charge neutrality. In this paper we further pursue this question by considering so-called exchange defects. These consist of a swap of a group II and a group IV atom, which we call an exchange

defect. First of all, we analyze how many "wrong" tetrahedra such an exchange defect produces. Secondly, we model a large supercell in which we make a number of exchange swaps. We study the behavior of the gap and states in the gap as functions of the distribution of the exchange defects and also compare these results with those of a fully random structure, as more specifically defined later. Finally we relate these results with those of the individual antisite defects which were recently studied.[11] In this study we focus on $ZnGeN_2$ because it has a larger gap than $ZnSnN_2$. In the local density approximation, the gap of $ZnSnN_2$ becomes very small and this makes it difficult to study the defect-related bands in the gap. However, the essential physics should be similar, so the main conclusions will transfer to the case of $ZnSnN_2$ as well.

II. METHODS AND MODELS

The calculations were done within the local density approximation (LDA) to density functional theory.[12–14] The full-potential linearized muffin-tin orbital method[15,16] was used for the solution of the Kohn-Sham equations and the band structures. The basis sets used and other details of the computation are the same as those reported in Ref. 11. Each structure was relaxed by a conjugate gradient method to find the closest local minimum for a given configuration.

We studied several supercells each consisting of 128 atoms, which is a $2 \times 2 \times 2$ supercell of the 16-atom primitive unit cell of $ZnGeN_2$, with various arrangements of exchange defects. While in a 128 atom cell there may still be significant defect-defect interactions especially when considering these somewhat extended defect complexes, we emphasize that in this study it is not our purpose to exclude such defect-defect interactions but precisely to include them. We are here not focused on the dilute limit of such defect complexes but on their effect on the overall band gap of the system, including the defect-defect interaction effects.

In Fig. 1 we illustrate the structure of a single exchange defect. One can see that in the perfect crystal structure each horizontal row has alternating blue (Zn) and pink (Ge) atoms. The single exchange defect shown in Fig. 1a corresponds to a swap of two nearest neighbor cations (connected to the same N) in the basal plane as indicated by the red line. As explained in the figure caption, this exchange defect leads to three (1,3) and three (3,1) "wrong" tetrahedra. A slightly different exchange defect can be made by swapping two atoms in neighboring planes as illustrated in Fig. 1 b-d. As the caption explains, this defect also has three (1,3) and three (3,1) tetrahedra. The same is true for more distant atom swaps. Once we start adding more exchange defects, the defective regions may start overlapping and the number of wrong tetrahedra per swap may be reduced. Specifically, we used three different structures each with two
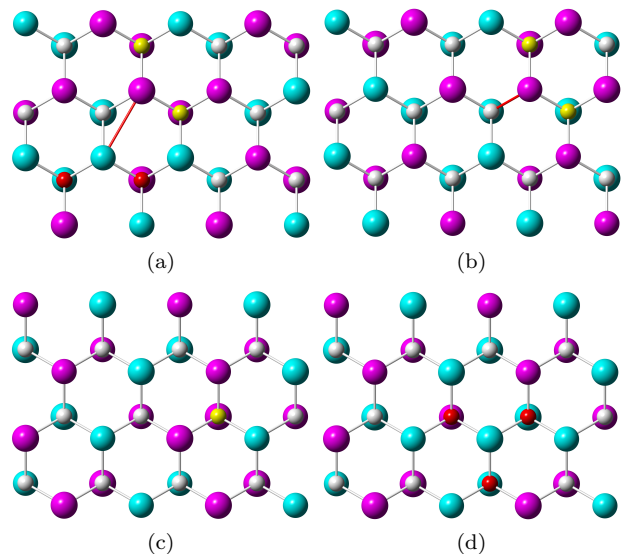

FIG. 1. (Color online) (a) Single exchange defect between atoms in the same basal plane. The blue and pink spheres indicate Zn and Ge, the small white spheres N. The red line indicates the swapped atoms. The yellow spheres indicate N surrounded by 3 Ge and 1 Zn (1,3) tetrahedron, the red spheres indicate N surrounded by 3 Zn and 1 Ge (3,1) tetrahedron. Additional (1,3) and (3,1) tetrahedra occur above each antisite. (b) Single exchange defect between near-neighbor Zn and Ge in adjacent planes (B and C); In (b), showing layers B on top of C, one can see two (1,3) tetrahedra indicated by the yellow N; In (c) (layers A on top of B) one can see a third (1,3) tetrahedron. In (d), showing layers C on top of D, one can see three (3,1) tetrahedra indicated by red N spheres.

exchange defects, which have respectively 4, 5 and 6 (1,3) and (3,1) tetrahedra. These structures are shown in Fig.2 and the statistics of their tetrahedra are listed in Table I along with other models and calculated properties.

Next, we used two different distributions of 3 swaps, one in which they were all close neighbors and the second in which we kept the Zn_{Ge} separated from the Ge_{Zn}. The latter was made by first occupying sites according to a random number generator, and next we swapped atoms by hand to keep the antisites from being near neighbors.

Finally, we also study a more fully random system. The latter is defined in terms of the special quasi-random structures (SQS) approach.[17] In the SQS approach, one constructs an ordered structure such that various pair-correlation functions and higher order correlation functions between spins a certain distance from each other agree as close as possible to the fully random distributions. Instead of considering pairs on the cation lattice, we consider the five possible tetrahedra around each N, (0,4), (1,3), (2,2), (3,1), (4,0), which in the fully random case should occur according to the binomial distribution, which for equal concentrations of the two cations means in the ratio 1/16, 4/16, 6/16, 4/16, 1/16. Using a search among various models with the 64 cation sites populated according to a random number generator, we found sev-
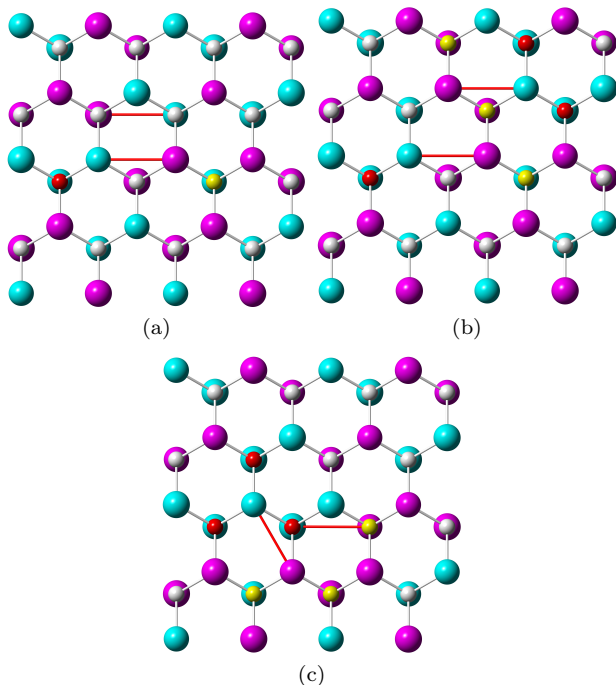
FIG. 2. (Color online) Three different models with two exchange defects each and respectively 4, 5 and 6 wrong tetrahedra in cases (a), (b), (c). The blue spheres indicate Zn, the pink Ge, the small spheres are N, with the yellow ones indicating a (1,3) and red ones a (3,1) tetrahedron.

eral cells that obey this distribution of tetrahedra and used a few of these as representative examples of a random system. This approach is equivalent to considering correlation functions with $k = 0, 1, 2, 3, 4$ up to nearest neighbors only. One could further improve on this SQS by requiring higher distance pairs etc. to have vanishing pair correlations.

We note that the charge neutrality is always conserved overall because we start from a stoichiometric sample and only make exchanges; we do not add or delete atoms of a given kind. So, the question now is how do these defects affect the band structure? In the following we define the band gap as the difference between the lowest empty state and the highest occupied states. For a disordered system, one also considers defect state tails below the band edges in the gap region. In amorphous systems, one often distinguishes a mobility gap, a gap above which states contribute actually to transport from a optical gap. We thus clarify that the gaps we consider here are related to optical absorption gaps and do not represent a mobility gap. On the other hand, we will also study the localization behavior of the states tailing into the nominal perfect crystal gap.

III. RESULTS

First, let us consider a single swap between nearest neighbor atoms in the same basal plane. The band structure and density of states for this case is shown in Fig. 3. We can see that some defect-like bands occur in the gap close to the VBM. These bands are filled because we consider the neutral charge state. This result is consistent with expectations from the individual defects.[11] In fact, a Zn_{Ge} antisite was shown to behave as an acceptor defect, while a Ge_{Zn} antisite behaves as a very shallow donor, essentially producing only a resonance in the conduction band with potentially a hydrogenic Coulomb tail bound state. The latter however is not reproduced in supercell calculations because of the limited size of the cell. In the present case, the donor electrons are transferred to the acceptor so the donor is in the positive state, compensating the negative acceptor. Hence the defect levels due to
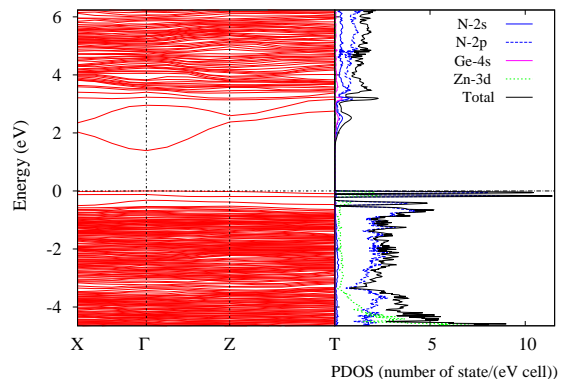

FIG. 3. (Color online) Band structure and density of states for single nearest neighbor swap exchange defect.

the Zn_{Ge} acceptor are all filled. Because the Zn_{Ge} acceptor is still relatively shallow (< 0.1 eV binding energy) although less shallow than the Ge_{Zn} donor, one would expect the gap to be only slightly reduced from the perfect crystal value. However, we find that the gap is reduced from 1.93 eV in the perfect crystal to 1.39 eV. These are LDA gaps and thus underestimated but are sufficient to explore the changes in gap upon introducing the exchange defects. The reason for the gap lowering becomes clear on closer inspection of the band structure and comparing it to the case of a single Zn_{Ge} antisite in Fig. 11 of Ref. 11. In the present case, there is a resonance in the conduction band due to the Ge_{Zn} antisite which pushes the conduction band minimum (CBM) down. Of course, in the dilute limit one would not expect this resonance to lower the conduction band but here we are concerned with the band structure of a 128 atom cell which has 32 Zn sites, so $1/32 = 3.125$ % concentration of Ge_{Zn} defects. Furthermore the Ge_{Zn} occurs close to the Zn_{Ge} site and in fact, as mentioned earlier there are actually six wrong

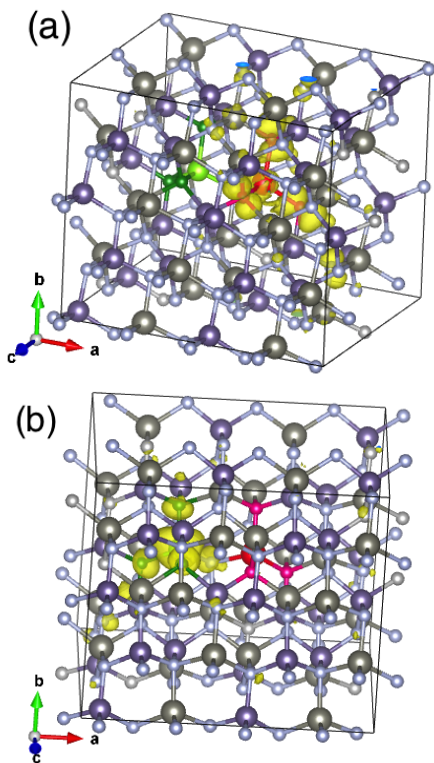tetrahedra, which already has a significant effect on both the VBM and CBM.

FIG. 4. (Color online) Wave function modulo squared for (a) the highest valence band and (b) the conduction band resonance in the model with one exchange defect. The grey and purple spheres indicate regular lattice sites Zn and Ge respectively, while the red indicates Zn_{Ge} and the green indicates Ge_{Zn}. The small green spheres indicate N surrounded by 3 Ge and one Zn, while the small red spheres indicate N surrounded by 3 Zn and one Ge.

Inspection of the wave functions shown in Fig. 4 corresponding to the defect levels just above the VBM shows that their wave functions are indeed localized near the Zn_{Ge} antisite and similar to those for an isolated antisite defect. Fig. 4 also shows the conduction band resonance near Ge_{Zn}.

The energy of formation of this single exchange defect is 2.8 eV compared to the perfect crystal. This is comparable to the energy of formation of the Zn_{Ge} isolated defect. The latter depends on chemical potential conditions, but here we compare only systems with the same number of Zn and Ge atoms, so we can directly compare the energy of the crystal with the exchange defect to that of the perfect crystal, without considering equilibrium with different reservoirs. Furthermore we consider the system to be overall neutral and this condition fixes the Fermi level at the highest occupied band.

For the alternative single swap defect considered in Fig.1b we found essentially identical results and therefore we do not show them here. Next, we consider several systems with 2 swaps as indicated in Fig. 2. These show similar band structures with some variation in the width of the distribution of Zn_{Ge} defect states near the VBM, as indicated by the gap shown for each structure in Table I. We also see from this table that the energy of formation tends to increase with the number of octet-rule-violating tetrahedra. Remarkably, however, the model with two swaps, shown in Fig. 2a has a lower energy of formation than the one-swap model. In view of the opposite charges of the Zn_{Ge}^{-2} and Ge_{Zn}^{+2} we may note that this configuration contains two nearby oppositely pointing dipoles, which helps to lower its energy. Still, it is remarkable that this arrangement would lower the energy enough to compensate for the fact that we have one more exchange defect.
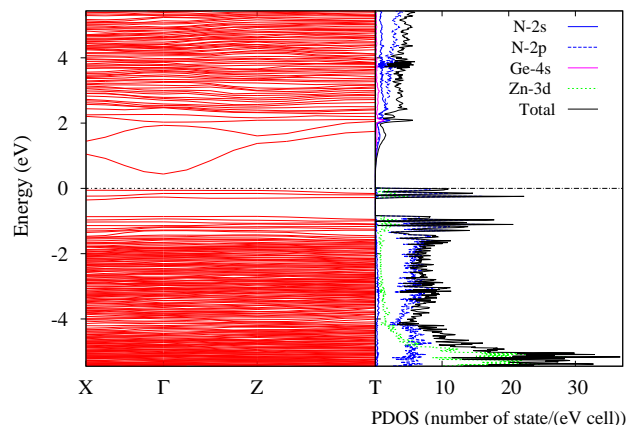

FIG. 5. (Color online) Band structure and density of states for 3 nearest-neighbor exchange defects for the model containing a (4,0) tetrahedron.

Next, we consider a system with three exchange defects, all of them occurring between near-neighbor Zn and Ge. As shown in Table I, in this case there occurs a (4,0) tetrahedron; in other words a N surrounded by four Zn atoms. The band structure and density of states, shown in Fig. 5, now exhibits a defect band, filled with electrons, well separated from the valence band maximum. Nominally, one could say that the gap is now significantly reduced because it corresponds to the gap between the defect band and the CBM. We will refer to this defect band as an intermediate band.

However, the flat dispersion and hence high effective mass will probably result in poor hole transport in this defect band. Inspection of the wave function (Fig. 6) shows that all three bands in the middle of the gap have states localized near the N surrounded by four Zn. This result is understandable because the defect states of Zn_{Ge} are mostly N-p like and the localized states of the N surrounded by all Zn will be more pushed up by the Zn-$3d$ states than other for N. The usual valence band below

TABLE I. Numbers of tetrahedra of different types in various models, their LDA band gaps, and energies of formation. The type of tetrahedron is indicated as (n_{Zn}, n_{Ge}) with n_{Zn} (n_{Ge}) the number of Zn (Ge) neighbors to each N.

model	(2,2)	(1,3)	(3,1)	(0,4)	(4,0)	E_{gap} (eV)	E_{for} (eV)	comment
1-swap	58	3	3	0	0	1.39	2.8	defect level close to VBM
2-swaps a	56	4	4	0	0	1.58	2.3	
2-swaps b	54	5	5	0	0	1.26	2.9	
2-swaps c	52	6	6	0	0	1.01	4.7	
3-swaps	47	9	7	0	1	0.50	7.4	intermediate band
separated 3 Zn_{Ge} and 3 Ge_{Zn}	41	10	12	0	0	0.44	10.5	reduced gap, raised VB
random	24	16	16	4	4	0.33[a]	20.0	

[a] LDA+U gap

the separated intermediate band still has states near its maximum that are localized near Zn_{Ge} but not on the N surrounded by four Zn.

As an aside, an intermediate band situation like this one, has been suggested to be possibly useful for photovoltaics. The idea is that if such a band is partially filled, optical transitions can occur between the VBM and this intermediate band, as well as between this intermediate band and the CBM. In addition to the usual VBM-CBM transitions, one could thus absorb photons of lower energy. If at the same time one can maintain the quasi-Fermi level of the n- and p-type sides of an interface near the nominal CBM and VBM then one could maintain an open-circuit voltage close to the value of the large band gap of the unperturbed material. However, this intermediate band can also act as a carrier trap. Thus good transport in this band, and optimal balance between these different absorption and capture processes is essential to make such a concept work for a more efficient solar cell. In the present case, the intermediate band is filled, although this situation could of course be changed by p-type doping or by going slightly off-stoichiometry toward a Zn-rich situation. However, more importantly, this structure seems to cost a substantial energy of formation. We do not have a decomposition of the total energy of formation in terms of different types of wrong tetrahedra but the N surrounded by four Zn could play a significant role in this. In any case, this kind of defect seems rather unlikely to occur.

Next, we consider a 128-atom cell also with three Zn_{Ge} and three Ge_{Zn} but with the antisites placed in a phase-separated manner in the structure. The statistics of different types of tetrahedra is again summarized in Table I. The band structure and density of states are shown in Fig. 7. In this case we now see that the gap between the defect band and the VBM has completely filled in and the gap is significantly reduced to 0.44 eV. This result means a lowering of the gap by 1.49 eV. Taking into account the corrections beyond LDA, and a gap of 3.4 eV for perfect crystal $Pna2_1$ $ZnGeN_2$, the gap would now be reduced to 1.9 eV.

The HOMO wave function for this "phase-separated" case is displayed in Fig. 8. One can indeed see that the Zn_{Ge} (indicated by red spheres) are separated spatially form the Ge_{Zn} (indicated by green spheres) in this model. The result shows again localization near the Zn_{Ge} defects but in contrast to the previous 3-swap model, the wave function now looks more extended. Its state percolates along a chain across the whole cell connecting various Zn_{Ge} sites. This percolation clearly would increase the band width of such defect bands and explains why the gap between the defect bands and the VBM fills in. Similar extended states can be seen for the HOMO-1 and HOMO-2 states. The CBM and CBM+1 states on the other hand have more weight near the Ge_{Zn} sites.

From the energies of formation in Table I we can see that this model has significantly higher energy than the near-neighbor exchange models with 3 swaps. Because these defects are of opposite charge in an overall neutral situation where the charge is transferred from the donors to the acceptors, one indeed expects this segregation to be unfavorable in total energy.

Finally, we consider a "fully" random system represented by a SQS constructed in the way discussed in the previous section. The structure of this model is shown in Fig. 9. Its band structure is shown in Fig. 10. We found that in this model the gap is zero in LDA. This means the gap is reduced by at least 1.9 eV. Therefore we use the LDA+U model used in Skachkov et al.[11] which in pure $ZnGeN_2$ in the $Pna2_1$ structure opens the gap to 3.4 eV. After relaxation of the structure, this results in a gap of 0.33 eV. This is a remarkable lowering of the gap by about 3.1 eV compared to the $Pna2_1$ structure. This in some sense confirms the similar results obtained for $ZnSnN_2$ by Feldberg et al.[6] who studied a special quasirandom structure (SQS) supercell to simulate the completely random placement of the Zn and Sn atoms and also found a significant reduction of the gap. The gap reduction found here is even more severe. Unfortunately, we have no detailed information on the statistics of the different types of tetrahedra in that previous study.

On the other hand, we find this structure to have an energy cost relative to $Pna2_1$ of 20 eV per 128 atom cell after relaxation. This large energy cost corresponds to the large number of antisites in this model. To put this in perspective, 20 eV/128 atom cell corresponds to 0.625 eV/formula unit or 60 kJ/mole or 14 kcal/mole. For comparison the energy of formation of $ZnGeN_2$ relative
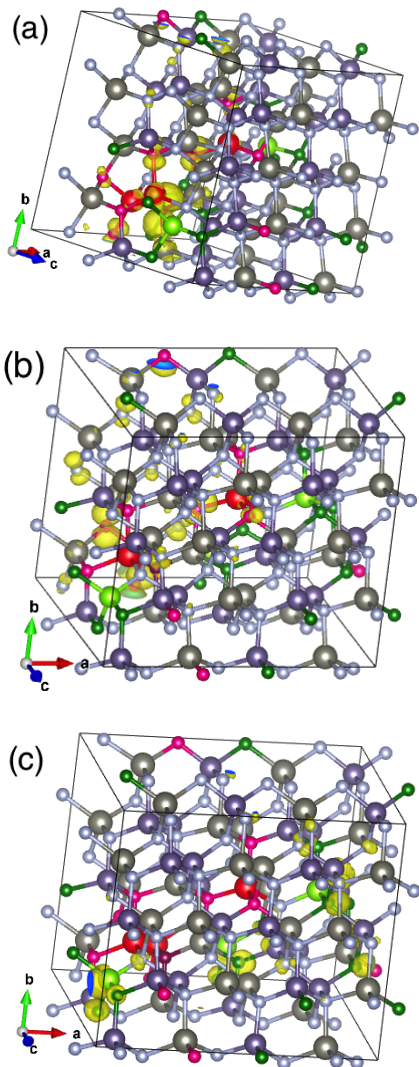
(a)

(b)

(c)

FIG. 6. (Color-online) Figure showing $|\psi|^2$ for the wave functions of a few selected states at $\mathbf{k} = 0$ in the 3-swap model. Panel (a) corresponds to the highest occupied or HOMO state of the model which lies at the top of the defect band. The bonds to Zn are indicated and show the wave function to be localized near a N surrounded by 4 Zn (dark red), two of them Zn_{Ge} (in red) and two of them regular lattice Zn. (b) shows the HOMO-3 or the highest valence band state below the intermediate band. This state is still localized near Zn_{Ge} but not on the N with 4 Zn. (c) shows the 2nd conduction band level which is a resonance located near the three Ge_{Zn} (green).

to the elemental solids Zn and Ge and N_2 molecules is -2.43 eV/formula unit. It shows that such structures are very unlikely or at least very far from equilibrium.
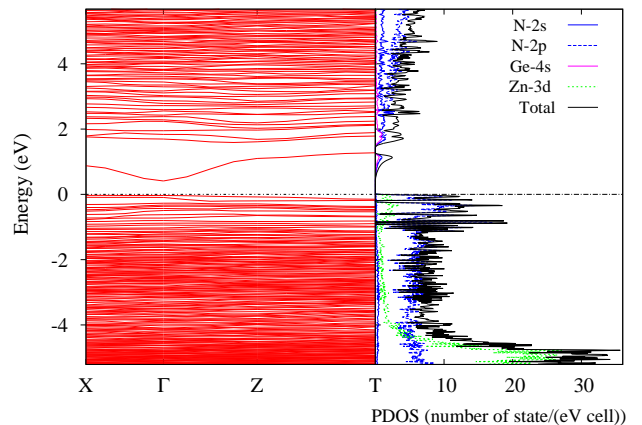

FIG. 7. (Color online) Band structure and DOS for $ZnGeN_2$ with three exchange defects with the Zn_{Ge} antisites spatially separated from the Ge_{Zn} antisites
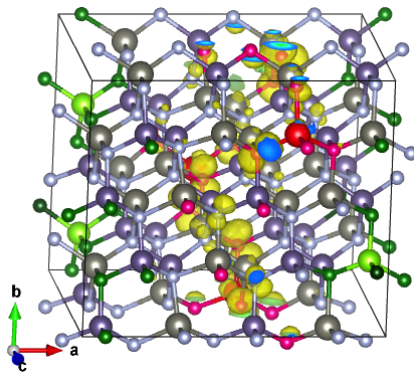

FIG. 8. (Color online) Wave function modulo squared for highest occupied band at Γ for the model with 3 swaps and "phase separated" Zn_{Ge}, Ge_{Zn}.

IV. CONCLUSIONS

We studied various models and degrees of randomness of $ZnGeN_2$. We found that a single exchange defect, *i.e.* exchanging a near neighbor Zn and Ge causes several charge-neutrality-violating tetrahedra and leads to a band structure which is characterized by a defect band close to the VBM and corresponding essentially to the Zn_{Ge} antisite acceptor levels broadened somewhat into a band. However, the CBM is also lowered by the occurrence of a Ge_{Zn}-related resonance in the conduction band. This single exchange defect already reduces the gap by about 0.5 eV. We found that when several such exchange defects occur they interact and tend to push the defect band deeper into the gap resulting in some cases in a distinct "intermediate band" situation. In particular we found this situation to occur when a N surrounded by four Zn atoms occurred in the structure. In a structure
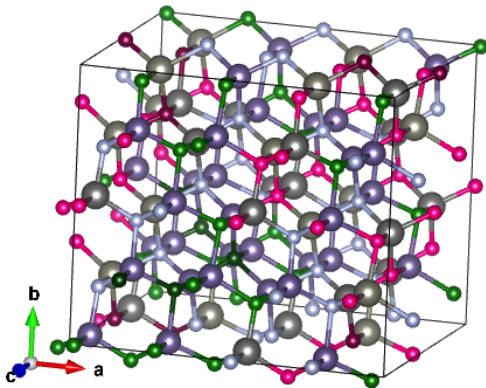
FIG. 9. (Color online) Structure of a 128 atom random placement model: the Nitrogen atoms are colored according to their nearest neighbors (n_{Zn}, n_{Ge}): (2,2) grey, (3,1) green (4,0) dark green, (1,3) red, (0,4) dark red.
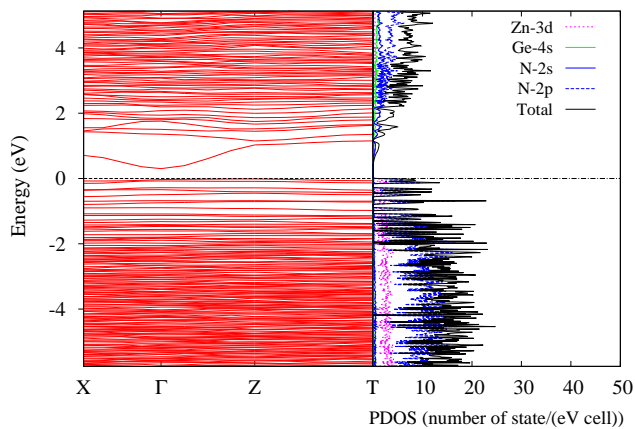

FIG. 10. (Color online) Band gap in relaxed random SQS 128 atom model for $ZnGeN_2$ in LDA+U.

with 3 exchange defects per 128 atom cell, corresponding to a concentration of 9.375 % phase separated from each other, already no separated defect bands were found but instead a reduction of the gap by a raising of the valence band. The gap was reduced by about 1.5 eV. Finally, in a completely random structure with a binomial distribution of the five different types of nearest neighbor tetrahedra, the gap was found to be reduced even further; by as much as 3 eV. We remind the reader that these are optical band gaps, not mobility gaps. On the other hand, it is also clear from our study of the localization of the states that for the more isolated exchange defects, the states in the band gap tail above the valence band edge are rather localized and hence conduction of holes in such states is only expected to proceed by a hopping model. A detailed study of transport properties and

an actual determination of the mobility gap is beyond the scope of this paper.

On the other hand the total energy of the system significantly increases with the number of exchange defects. The energy cost is of order 2.8 eV per exchange defect. When doubling the number of exchange defects, the energy of formation roughly doubles if the defects occur independent of each other (case 2-swaps c in Table I) but can be significantly reduced when these exchange defects occur close to each other so that the total number of octet-rule violations is reduced. The model with 3 swaps has indeed about 3 times the energy of formation of 1 swap but when the antisites are kept phase-separated the energy of formation is higher. The energy increases from 2.5 eV per swap if they are kept close to each other, to 3.5 eV if they are kept apart in the 3-swap model. A fully random structure has even higher energy of formation; of order 0.625 eV per formula unit.

In our previous paper[11] we found that antisite defects Zn_{Ge} and Ge_{Zn} are the most energetically favorable point defects in $ZnGeN_2$ and compensate each other, thereby pinning the Fermi level. Because of their opposite charge, they will also attract each other and therefore one might expect them to form near-neighbor exchange defects. However, the equilibrium concentration of the antisite defects is low; of order 10^{16} cm^{-3}. Here we find that when such defects occur in pairs in large concentrations, they can lower the band gap. For a 3 % concentration of exchange defects, which is of order 0.7×10^{21} cm^{-3}, the gap is reduced by about 0.5 eV. For higher concentrations of order 9 % (or 2.1×10^{21} cm^{-3}) the gap may be reduced by as much as 1.5 eV. We find that the exchange defects will tend to cluster rather than phase separate, as the antisites forming them have opposite charge and attract each other. Nonetheless, we can see that the defect concentrations considered here are quite high compared to equilibrium concentrations. Thus we expect such band gap lowering due to disorder only when the growth is significantly perturbed and far from equilibrium. Under highly non-equilibrium circumstances it is unlikely that high quality crystallinity can be maintained.

Although we primarily focused on $ZnGeN_2$, we also performed some calculations for $ZnSnN_2$ and found also very strong gap reductions under similar circumstances. Because in LDA the gap is very small to begin with, the $ZnSnN_2$ gap with exchange defects essentially closes and this makes it difficult to study the effects in detail without going beyond LDA. Nonetheless we anticipate the general conclusions to be applicable also to $ZnSnN_2$.

[1] W. R. L. Lambrecht and A. Punya, in *III-Nitride Semiconductors and their Modern Devices*, edited by B. Gil (Oxford University Press, 2013) Chap. 15, pp. 519–585.

[2] L. Zhu, P. Maruska, P. Norris, P. Yip, and L. Bouthillette, MRS Internet J. Nitride Semicond. Res. **4S1**, G3.8 (1999).

[3] K. Du, C. Bekele, C. C. Hayman, J. C. Angus, P. Pirouz, and K. Kash, J. Cryst. Growth **310**, 1057 (2008).

[4] L. Lahourcade, N. C. Coronel, K. T. Delaney, S. K. Shukla, N. A. Spaldin, and H. A. Atwater, Advanced Materials **25(18)**, 2562 (2013).

[5] N. Feldberg, B. Keen, J. D. Aldous, D. Scanlon, P. A. Stampe, R. Kennedy, R. Reeves, T. D. Veal, and S. Durbin, in *Photovoltaic Specialists Conference (PVSC), 2012 38th IEEE* (2012) pp. 002524–002527.

[6] N. Feldberg, J. D. Aldous, W. M. Linhart, L. J. Phillips, K. Durose, P. A. Stampe, R. J. Kennedy, D. O. Scanlon, G. Vardar, R. L. Field, T. Y. Jen, R. S. Goldman, T. D. Veal, and S. M. Durbin, Appl. Phys. Lett. **103**, 042109 (2013).

[7] P. C. Quayle, K. He, J. Shan, and K. Kash, MRS Communications **3**, 135 (2013).

[8] P. C. Quayle, E. W. Blanton, A. Punya, G. T. Junno, K. He, L. Han, H. Zhao, J. Shan, W. R. L. Lambrecht, and K. Kash, Phys. Rev. B **91**, 205207 (2015).

[9] M. Maunaye and J. Lang, Mater. Res. Bull **5**, 793 (1970).

[10] E. Blanton, K. He, J. Shan, and K. Kash, in *Symposium E/H Photovoltaic Technologies, Devices and Systems Based on Inorganic Materials, Small Organic Molecules and Hybrids*, MRS Proceedings, Vol. 1493 (2013) pp. 237–242.

[11] D. Skachkov, A. Punya Jaroenjittichai, L.-y. Huang, and W. R. L. Lambrecht, Phys. Rev. B **93**, 155202 (2016).

[12] P. Hohenberg and W. Kohn, Phys. Rev. **136**, B864 (1964).

[13] W. Kohn and L. J. Sham, Phys. Rev. **140**, A1133 (1965).

[14] U. von Barth and L. Hedin, Journal of Physics C: Solid State Physics **5**, 1629 (1972).

[15] M. Methfessel, M. van Schilfgaarde, and R. A. Casali, in *Electronic Structure and Physical Properties of Solids. The Use of the LMTO Method*, Lecture Notes in Physics, Vol. 535, edited by H. Dreyssé (Berlin Springer Verlag, 2000) p. 114.

[16] T. Kotani and M. van Schilfgaarde, Phys. Rev. B **81**, 125117 (2010).

[17] A. Zunger, S.-H. Wei, L. G. Ferreira, and J. E. Bernard, Phys. Rev. Lett. **65**, 353 (1990).